ACS APPLIED MATERIALS & INTERFACES

Research Article

www.acsami.org

Highly Ordered Self-Assembling Polymer/Clay Nanocomposite Barrier Film

Ray Cook,[†] Yihong Chen,[†] and Gary W. Beall*[,†,‡]

[†]Materials Science, Engineering and Commercialization Program, Texas State University, San Marcos, Texas 78666, United States

[‡]Physics Department, Faculty of Science, King Abdulaziz University, Jeddah 21589, Saudi Arabia

ABSTRACT: Efforts to mimic complex-structured biologically based materials such as abalone shell have occupied substantial research time and effort in science and engineering. The majority of the efforts involve tedious and expensive techniques and processes. Layer-by-layer (LBL) is one such technique that can produce materials with quite unique physical properties, approaching, and in some cases surpassing, those seen in nature. The LBL technique, however, is quite tedious and difficult to implement commercially. We report here the discovery of an organic/inorganic spontaneous self-assembling system that forms a highly structured nanocomposite. The driving force behind this self-assembly appears to be entropy. This discovery should open up completely new avenues to designing hierarchical composites and structures. The films have been studied by X-ray diffraction and the barrier properties for oxygen diffusion measured.

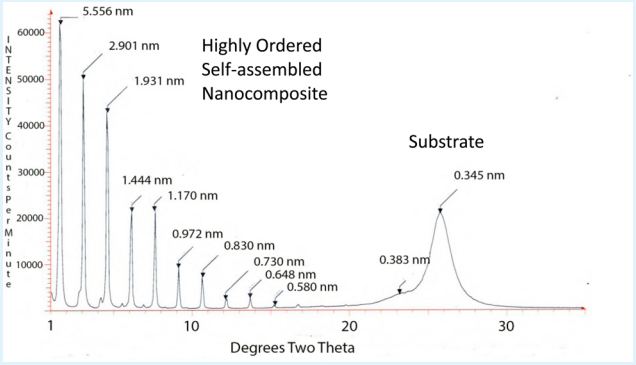

KEYWORDS: *biomimetic, nanocomposite, gas barrier, self-assembly, highly ordered*

INTRODUCTION

Biomimetics is a fascinating area that brings materials science and biology together to produce unique materials that attempt to copy biological systems.[1,2] Biologists have documented a number of systems that exhibit highly ordered structures mediated by biological mechanisms that control their assembly many times at the nanoscale. There are numerous biologically derived materials that exhibit unusual physical and mechanical properties.[3−6] One such material is abalone shell, where very precisely sized layers of platy aragonite crystals are surrounded by protein in a very ordered way.[7,8] The aragonite plates are arranged like bricks in a brick wall, with the protein acting as the mortar. This kind of inorganic/organic composite yields material that has outstanding toughness and tensile strength. The fracture toughness of abalone shell has been reported to be 3000 times greater than that of monolithic calcium carbonate.[9]

There has been a great deal of interest in developing techniques to mimic these types of structures, especially on the nanoscale. One approach that has been utilized extensively is the layer-by-layer (LBL) process.[10] In the LBL process, the layering that occurs in biological systems is mimicked by mechanical building of the structure sequentially layer by layer. In the simplest approach, a substrate is repeatedly dipped in solutions of polymer followed by platy nanoparticle dispersions to build up as many as 50 alternating organic/inorganic layers. Normally between each dipping there are rinsing and drying steps. This approach is tedious and produces substantial amounts of waste rinsewater. These problems render the LBL technique expensive and difficult to implement on a commercial scale. This technique, however, can produce films with outstanding properties such as high strength and outstanding gas barrier properties and impart flame retardancy to coated substrates. Kotov et al. have reported transparent thin films prepared with clay and poly(vinyl alcohol) (PVOH) that yield a modulus of 100 GPa and a tensile strength of 400 MPa.[11] This "plastic steel" is a result of the unique nanobrick wall architecture that is only possible with LBL assembly. These films are also quite transparent. It has been reported that LBL films produced with chitosan and vermiculite yield films that exhibit very high barrier properties to oxygen of 0.009 $cm^3/m^2 \cdot day \cdot atm/mil$.[12] It has been demonstrated that substrates such as linen coated with LBL films become much more flame-retardant.[13] As stated before, these highly ordered LBL films come at the price of arduous processing steps and substantial waste generation. We report here a technique and system that is self-assembling at the nanoscale but bridges to the micron scale, which eliminates the problems encountered with traditional LBL assembly. The structure has been studied by X-ray diffraction, and the barrier properties for oxygen permeability have been measured.

MATERIALS AND METHODS

Ink Solutions. All solutions of the polymers and montmorillonite (MMT) were prepared by dispersing weighed amounts of the

Received: March 12, 2015
Accepted: May 6, 2015
Published: May 6, 2015

ACS Publications © 2015 American Chemical Society

DOI: 10.1021/acsami.5b02162
ACS Appl. Mater. Interfaces 2015, 7, 10915−10919

compounds into deionized water with stirring for 24 h. Poly(vinylpyrrolidone) (PVP; K-15) was obtained from International Specialty Products Technologies Inc., poly(vinyl alcohol) (PVOH; mol wt of 77−79K and 99.998% hydrolyzed) was obtained from J. T. Baker, poly(ethylene oxide) (PEO; under the trade name polyox with a mol wt of 100000) was obtained from Dow Chemical, and MMT (Cloisite Na+) was donated by Southern Clay Products. All reagents were utilized as received from the suppliers.

Printing of Films. The solutions of the individual polymers and MMT were placed in Fujifilm Dimatix DMC-11601 print heads. It is a two-part cartridge consisting of a reservoir and a print head. The nozzle plate is located on the bottom of the print head and is made of silicon. It contains 16 nozzles spaced 254 μm apart. Each nozzle is approximately 20 μm in diameter. It can generate drop volumes as small as 1 pL. All solutions were printed onto standard 8.5 in. × 11 in. CG5000 film sheets sold by 3M. These poly(ethylene terephthalate) (PET) films are manufactured by DuPont and are used primarily for transparencies in ink-jet and laser printers. The transparencies are coated with a water-soluble coating to promote ink adherence to the surface. This coating was removed prior to printing, utilizing a rinse with isopropyl alcohol.

After the solution had been inserted into the printer cartridge, it was taken to the printer for testing. The printer used was a DMP 2831 Dimatix Materials printer, which is used by developers of printable functional fluids and research and development. The printer was programed to print six 6.35 cm × 6.35 cm squares. The first layer was printed with the polymer of interest followed by printing over the same area with MMT dispersion. This is referred to as a bilayer. In each successive bilayer, one square was not printed on, so that by the sixth bilayer, only one square contained six bilayers.

Film Characterization. After all films had been printed, it was necessary to both examine them visually and test their permeability. The following methods were used to analyze the various films: optical microscopy, scanning electron microscopy, and permeability testing. The single-material PVP and MMT clay films were analyzed for permeability and using an optical microscope. Only those samples that contained layered solutions and clay were analyzed using a scanning electron microscope.

Optical Microscopy. The fiducial camera on the printer, while useful for visualizations during printing, was limited in ability to 5× scope. Therefore, each sample was viewed using an Olympus BX60 polarizing optical microscope. Each sample was viewed using polarized light at 5×, 10×, 20×, and 50× magnification. Polarized light helped to distinguish the difference between the polymer and clay layers. The different levels of magnification allowed for the identification of drop spacing. It also provided a visual for how well the solution dispersed over the substrate and whether any voids had developed.

Profilometry. Initially, to gauge the film thickness, samples were mounted on a Tencor Alpha Step 500 surface profilometer. A profilometer has a sensitive stylus that can indicate the surface profile. First, a sheet of Mylar alone was measured to gauge the substrate thickness. Then, different samples at varying numbers of layers were measured. This was done to see whether the layer growth (thickness) was linear or nonlinear.

Scanning Electron Microscopy (SEM). The next round of visual characterization involved viewing samples with an FEI Helios Nano Lab 400 scanning electron microscope. It was thought that SEM could assist in determining the film thickness. Because SEM causes the polymer to charge up, the image quality was degraded. To combat this, a 2 μm layer of gold was placed on the tops of the films so that an SEM image could be taken. This allowed for the films to be imaged.

Ion milling was performed utilizing SEM. On the basis of a user input pattern, SEM bombards the sample with ions, milling out a place where elemental analysis can be performed at user-programmed points. This shows the elemental composition at each measured point. This allowed for identification of where the transitions from gold to the film and the film to the substrate occur. This information can be used to determine the thicknesses of the different layers.

Permeability Study. Permeability measurements were taken for each sample containing a clay layer. A Mocon Ox-Tran 2/60 analyzer was used to perform permeability analysis and is capable of analyzing six samples at a time. This allowed for all six samples of each film (PVP/MMT, PVOH/MMT, and PEO/MMT clays) to be placed in the machine at the same time.

Wide-Angle X-ray Scattering (WAXS). X-ray analysis was conducted using a Bruker D8 focus powder X-ray diffractometer with a Sol-X solid state detector. A half-inch square section of each film was cut and glued to the sample holder with rubber cement. The samples were mounted with the printed films facing up. The selected scanning angle was from 1 to 35°.

Characterization of the Film Thickness. The thicknesses of the films were assessed in several different ways including SEM, optical microscopy, and by mass.

RESULTS AND DISCUSSION

The original premise behind this work was that ink-jet printing would be a commercially viable way to produce coatings that could deliver films that mimic LBL films. The plan was to print alternating layers of polymer and platy nanoparticles that would eliminate the rinsing and drying steps yet still yield the outstanding properties exhibited by LBL films. In order to eliminate the rinsing step, the byproduct of the interaction between the nanoparticle and polymer must be easily removed by evaporation. This criteria is fulfilled by several water-soluble polymers that interact with smectic clays via ion-dipole bonding, with the byproduct being water. In this work, dilute solutions (0.1−0.2% by weight) of PVP, PVOH, and poly(ethylene glycol) (PEG) individually were utilized as inks to print the polymer layer. A dispersion of sodium montmorillonite (0.2% by weight) was utilized as an ink to print the nanoparticle layer. One layer of polymer and one layer of clay are referred to as a bilayer. An ink-jet printer was utilized to produce films on PET substrates. The three polymers were chosen because they are all water-dispersible and are known to intercalate into MMT via ion-dipole bonding.[14] In this intercalation process, the polymers must uncoil in order to enter the confined space of the gallery. This causes a decrease in the entropy of the polymer. This decrease in entropy is offset by the entropy increase for thousands of water molecules that are displaced by the polymer ion-dipole bonding to the exchangeable cations on the surface of the clay in the gallery. MMT was chosen because of its high aspect ratio. A typical MMT will have a primary particle thickness of approximately 1 nm but will be greater than 100 nm in the other two dimensions. This platy structure, if arranged in an orderly fashion, presents a very good barrier to gas transport. Additionally, the polymers and MMT are also considered to be generally recognized as safe by the Federal Drug Administration, which is important because one of the interesting potential applications for these films would be food packaging. To form the films, an initial polymer layer was printed on a 6.35 cm^2 area followed by a similar layer utilizing the MMT dispersion, and this structure is referred to as one bilayer. Table 1 contains the average thickness of the various films varying from one to six bilayers measured with optical microscopy, SEM, and profilometry. Figure 1 contains an SEM image of a trench that has been cut by a gallium focused-ion beam. The thickness of one bilayer can clearly be seen and measured. Measurement of the layer was confirmed compositionally by using energy-dispersive analysis of X-rays (EDAX). Each bilayer is approximately 2−3 μm thick. Figure 2 contains the X-ray diffraction pattern of six bilayers of a film printed utilizing PVOH and MMT. It can be seen that the most prominent features in the X-ray pattern are two broad peaks

DOI: 10.1021/acsami.5b02162
ACS Appl. Mater. Interfaces 2015, 7, 10915−10919

Table 1. Film Thicknesses for Ink-Jet-Printed Films of Three Polymers and MMT Varying from One to Six Bilayers

	film thickness, μm		
bilayer	PVP and MMT	PVOH and MMT	PEG and MMT
1	3.92	2.90	3.50
2	5.39	4.35	4.50
3	7.84	6.77	7.00
4	10.78	9.19	10.50
5	13.23	11.60	13.00
6	15.19	13.54	15.00

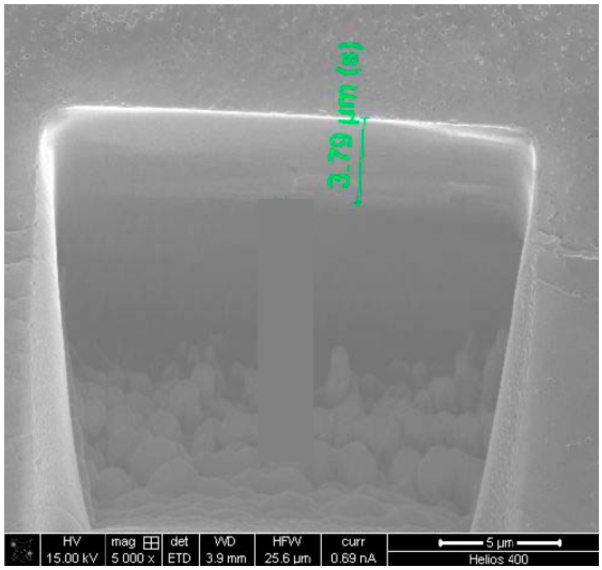

Figure 1. SEM image of a trench cut utilizing a gallium focused-ion beam that clearly shows the thickness of one printed bilayer on the PET substrate.

centered around 2θ = 26°; d spacings of 0.377 and 0.343 nm arise from the PET substrate. The only other feature is a weak broad peak centered around 2θ = 6.2°, with a d spacing of 1.42 nm that corresponds to hydrated MMT basal spacing. It appears that no intercalated complex between MMT and PVOH exists in these films. The intensity, broadness, and position of the peak indicate that the intercalated complex does not exist because normally one layer of polymer intercalated into the gallery would yield a d spacing in the range of 1.7−1.8 nm. It therefore appears that very little intercalation has occurred and the layers are distinct polymer and clay. Figure 3

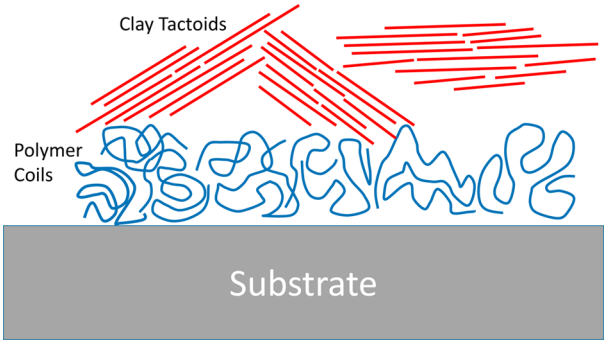

Figure 3. Schematic representation of one bilayer of polymer/clay exhibiting no intercalation.

contains a schematic representation of this structure. It can be seen that the polymer layer consists of coiled polymer chains and the clay layer exists as jumbled tactoids with no intercalation or mixing of the polymer and clay nanoparticles. The results for PEO and MMT are identical with those presented for PVOH.

The case with PVP and MMT is strikingly different. Figure 4 contains the X-ray diffraction pattern for a three-bilayer film produced utilizing PVP and MMT inks. The peak at around 2θ = 26° from the PET is still present, but a series of sharp and intense peaks starting at a spacing of approximately 5.6 nm dominate the pattern. This series of peaks is on the order of the 001 basal spacing, and 12 orders can be discerned. The sharpness, intensity, and number of reflection orders observed indicate that not only has the polymer intercalated the clay but the complex is extremely ordered and in almost perfect registry. In over 2 decades of research on polymer/clay nanocomposites, no such level of ordering has ever been observed. This basal spacing is consistent with experimental and molecular modeling that would indicate that there are approximately four layers of

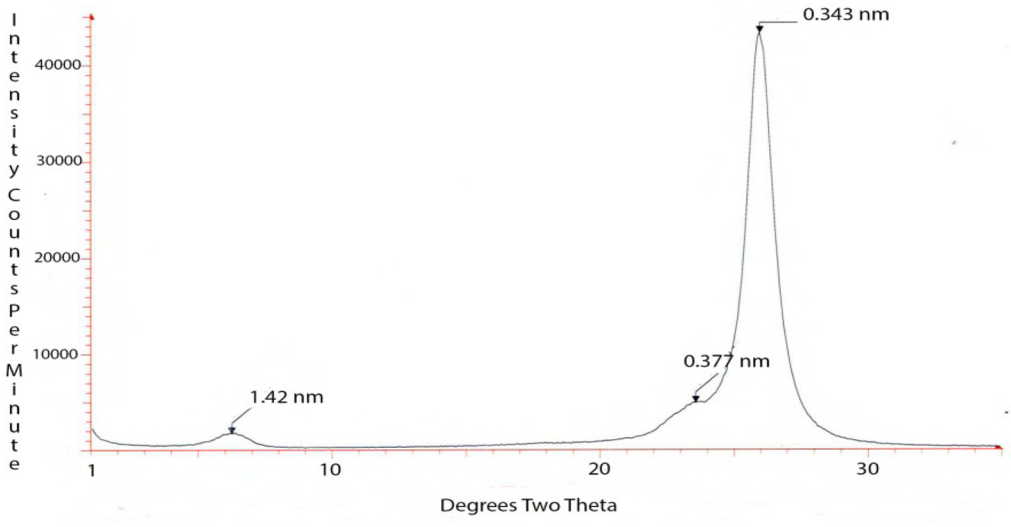

Figure 2. WAXS pattern of a six-bilayer film of PVOH and MMT on a PET substrate.

DOI: 10.1021/acsami.5b02162
ACS Appl. Mater. Interfaces 2015, 7, 10915−10919

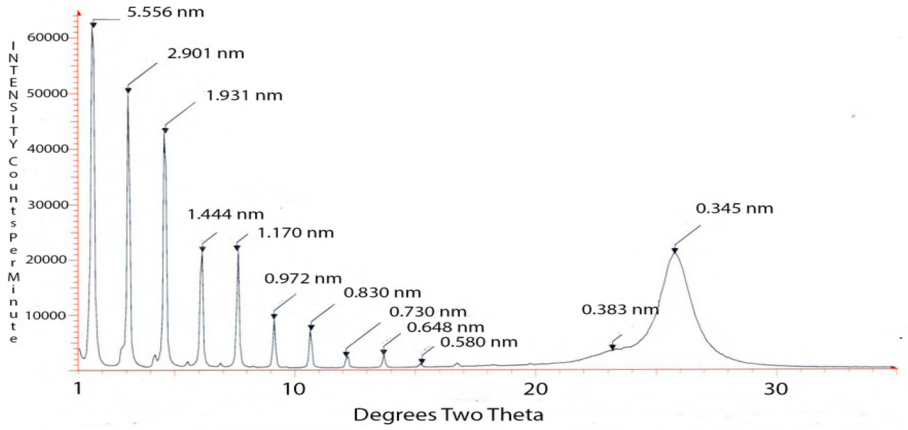

Figure 4. WAXS X-ray pattern of a three-bilayer composite of PVP and MMT.

PVP in the gallery.[14] Figure 5 contains a schematic representation of this structure. It can be seen that the polymer

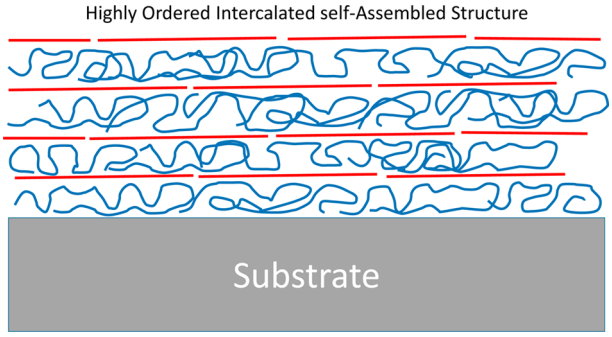

Figure 5. Schematic of the highly ordered intercalated nanostructure formed between PVP and MMT via self-assembly.

has completely intercalated the clay and formed a highly ordered nanocomposite. This structure appears to bridge across length scales from nanometers to microns. One result of this highly ordered composite should be a large decrease in gas permeation through the film. When the films were measured for the oxygen transmission rate (OTR), the PVP/MMT self-assembled nanocomposite yielded superior oxygen barrier results. Figure 6 gives a comparison of the OTR for PVOH/MMT, PEO/MMT, and PVP/MMT films with varying thicknesses from one to six bilayers. The level of the OTR

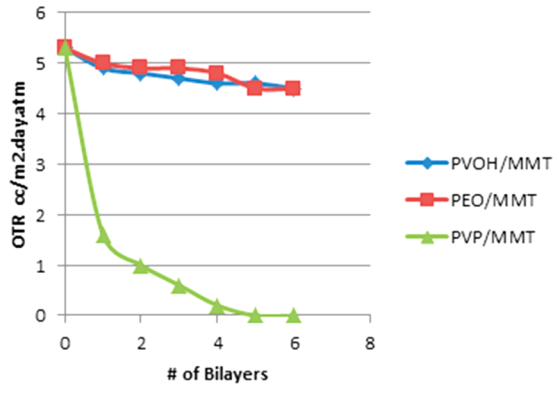

Figure 6. Comparison of the OTR for films printed with PVOH/MMT, PEO/MMT, and PVP/MMT at various thicknesses.

exhibited by only five bilayers of PVP/MMT was superior to metalized PET, which is the gold standard in barrier films. Equivalent thickness films of PET coated with just PVP or MMT alone yielded OTR values that were statistically indistinguishable from uncoated PET. It would appear that this unique spontaneous self-assembly and ordering arises from three main factors. The first involves the character of the polymers. PVP has a bulky pyrrolidone side group and is not able to form a tightly coiled conformation in solution as readily as PVOH and PEO. Therefore, there is less conformation energy needed to go from the coiled state to the more linear and confined intercalated state. All of the polymers will form intercalates with MMT via ion-dipole bonding. However, the three polymers bond differently when intercalating into MMT. The PVOH and PEO are both flexible enough that they can bond across the gallery and essentially glue the plates together, forming an intercalated complex that has only one molecule of polymer between the plates. It is almost impossible to form even a bilayer of polymer in the gallery of MMT with PVOH or PEO.[14] In contrast, PVP, when bonded to the cation on the clay surface, forces the adjacent pyrrolidone side groups into sterically hindered positions that make it difficult, if not impossible, to bond to the adjacent plate. This effect has been modeled previously with force-field-based modeling.[14] The second factor that is the energy driver for this process is entropy. In MMT, the exchangeable cation on the surface has a substantial partial positive charge that is normally accommodated by approximately three water molecules of hydration per sodium cation. The enthalpic energy of water ion-dipole-bonded to the sodium is similar to the energy of the bond formed between the carbonyl on the pyrrolidone group. The real energy difference comes in the entropy increase that occurs when the three water molecules are displaced by the intercalating PVP molecule. Assuming that about every third pyrrolidone group bonds to the surface, a PVP molecule with a molecular weight of 15000 would displace over 150 mol of water for each 1 mol of polymer. Therefore, the entropy decrease experienced by PVP in uncoiling will be swamped by the entropy increase experienced by the hundreds of water molecules that are displaced. The third factor is that ink-jet printing most likely contributes to the high degree of ordering because of surface tension effects that occur as the drops impact the surface and begin to evaporate. The new insight gained in this research could lead to the design of many new self-assembling systems. The recognition of the role of entropy in

DOI: 10.1021/acsami.5b02162
ACS Appl. Mater. Interfaces 2015, 7, 10915−10919

the intercalation could lead to combinations of polymers or copolymers and small molecules other than water that could strongly impact the types of self-assembling structures that can be designed. It could also open new possibilities for the design of more complex hierarchical structures because the polymer and nanoparticles spontaneously assemble.

CONCLUSIONS

It appears that in many cases ink-jet printing is not a viable route to supplant LBL techniques. This certainly is the case with PVOH and PEG in combination with MMT. It, however, has been discovered that in some cases a spontaneously self-assembling system will produce a highly ordered intercalated nanocomposite when utilizing an ink-jet printer. The intercalation is driven by entropy. These structures are ordered on the nanoscale but bridge across the micron scale in terms of the film thickness. The films yield coatings that exhibit a better oxygen barrier than metalized PET yet are transparent. The insights gained in this research could lead to the identification of other systems that will spontaneously self-assemble into ordered structures. Further work is necessary to determine if other printing or coating methods can be utilized to produce these highly ordered composite films.

AUTHOR INFORMATION

Corresponding Author

*E-mail: gb11@txstate.edu.

Author Contributions

The manuscript was written through contributions of all authors. All authors have given approval to the final version of the manuscript. These authors contributed equally.

Notes

The authors declare no competing financial interest.

ACKNOWLEDGMENTS

This research was supported by the National Science Foundation (PREM Center for Interfaces; Grant DMR-1205670) and the Robert A. Welch Foundation (Grant AI-0045).

REFERENCES

(1) Sarikaya, M. An Introduction to Biomimetics: a Structural View Point. *Microsc. Res. Technol.* **1994**, *27*, 371−377.

(2) Srinivasan, A. V.; Haritos, G. K.; Hedberg, F. L. Biomimetics: Advancing Man-made Materials through Guidance from Nature. *Appl. Mech. Rev.* **1991**, *44*, 463−476.

(3) Vincent, J. F. V. *Structural Biomaterials*; Princeton University Press: Princeton, NJ, 1991.

(4) Baer, E.; Hiltner, A.; R, J.; Morgan, R. J. Biological and Synthetic Hierarchical Composites. *Phys. Today* **1992**, 60−67 (Oct).

(5) Heuer, A. H.; Fink, D. J.; Laraia, V. J.; Arias, J. L.; Calvert, P. D.; Kendall, K.; Messing, G. L.; Blackwell, J.; Rieke, P. C.; Thompson, D. H.; Wheeler, A. P.; Veis, A.; Caplan, A. J. Innovative Materials Processing Stratagies: a Biomimetic Approach. *Science* **1992**, *255*, 1098−1105.

(6) Laraia, J. V.; Heuer, A. H. J. Novel Composite Microstructure and Mechanical Behavior of Mollusk Shell. *Am. Ceram. Soc.* **1989**, *72*, 2177−2187.

(7) Fritz, M.; Belcher, A. M.; Radmacher, M.; Walters, D. A.; Hansma, P. K.; Strucky, G. D.; Morse, D. E. Flat Pearls from Biofabrication of Organized Composites on Inorganic Substrates. *Nature* **1994**, *49*, 49−51.

(8) Lin, A.; Meyers, M. A. Growth and Structure in Abalone Shell. *Mater. Sci. Eng., A* **2005**, *390*, 27−41.

(9) Jackson, A. P.; Vincent, J. F. V.; Turner, R. M. A physical model of nacre. *Compos. Sci. Technol.* **1989**, *36* (8), 255−266.

(10) Decher, G.; Schlenof, J. B. *Multilayer Thin Films: Sequential Assembly of Nanocomposite Materials*; Wiley-VCH Verlag GmbH & Co.: Weinheim, Germany, 2012.

(11) Kotov, N. A.; Dekany, I.; Fendler, J. H. Layer-by-Layer Self-Assembly of Polyelectrolyte−Semiconductor Nanoparticle Composite Films. *J. Phys. Chem.* **1995**, *99* (35), 13065−13069.

(12) Guin, T.; Krecker, M.; Hagen, D. A.; Grunlan, J. C. Thick Growing Multilayer Nanobrick Wall Thin Films: Super Gas Barrier with Very Few Layers. *Langmuir* **2014**, *30*, 7057−7060.

(13) Li, Y. C.; Schulz, J.; Mannen, S.; Delhom, C.; Condon, B.; Chang, S.; Zammarano, M.; Grunlan, J. C. Flame Retardant Behavior of Polyelectrolyte−Clay Thin Film Assemblies on Cotton Fabric. *ACS Nano* **2010**, *4*, 3325−3337.

(14) Beall, G. W.; Powell, C. E. *Polymer−Clay Nanocomposites*; Cambridge University Press: Cambridge, U.K., 2011.

DOI: 10.1021/acsami.5b02162
ACS Appl. Mater. Interfaces 2015, 7, 10915−10919